Journal of Thermal Analysis and Calorimetry, Vol. 87 (2007) 1, 255–258

THERMAL ANALYSIS OF Fe(Co,Ni) BASED ALLOYS PREPARED BY MECHANICAL ALLOYING

A. González, J. Bonastre, L. Escoda and J. J. Suñol[*]

EPS, Campus Montilivi s/n, University of Girona, 17071 Girona, Spain

In this work several Fe(Co,Ni) based nanocrystalline alloys were obtained by mechanical alloying. Thermal study was performed by differential scanning calorimetry and thermogravimetry. After 80 h milling, all DSC scans show several reactions on heating. At low temperature, about 400 K, the exothermal process detected is associated to structural relaxation. In all alloys, the main crystallization process begins over 700 K and has apparent activation energy values between 3.7 and 3.1 eV at^{-1}. The Co content increases the thermal stability of this process. Furthermore, thermomagnetic measurements confirm the Co solid solution into Fe. The ferromagnetic–paramagnetic transition occurs at about 900 K.

Keywords: *apparent activation energy, Fe(Co,Ni) based materials, mechanical alloying*

Introduction

Mechanical alloying (MA) represents a non-expensive versatile route able to produce equilibrium as well as non-equilibrium materials including amorphous, nanostructured, composites, and extended solid solution systems [1–4]. During mechanical alloying, powder particles are subjected to severe mechanical deformation and are repeatedly deformed, cold-welded and fractured. The resulting fresh surfaces help re-aggregation of the powdered components with the formation of new particles, where the elements become stacked in layers, then allowing diffusion of one into the others.

Over the last decades, amorphous and more recently nanocrystalline materials have been investigated for applications in magnetic devices requiring magnetically soft materials [5]. Amorphous Fe–Zr–B and Fe–Nb–B alloys containing bcc-Fe nanocrystallites are of interest as soft magnetic materials [6–8]. The substitution of small amounts of Co or Ni for Fe in Fe-based magnetic materials generally results in an increase of saturation magnetization [9, 10]. Furthermore, it is known that the use of Ni favors the development of metastable structures at low milling times [11]. Among the different routes to produce these materials, MA allows producing alloys in large quantities but the process induces internal strain and impurities in the milled powders which need to be controlled to understand the magnetic properties [12]. In addition MA powders can be compacted and consolidated to complex shapes [13] whereas the materials developed by other techniques are mostly obtained in the form of ribbons and wires [5, 14].

The purpose of this study is an attempt to obtain nanocrystalline (Fe,Co,Ni)–Zr–B alloys by the ball milling technique, to establish the thermal stability and to analyze the effect of partial substitution of Fe by Co.

Experimental

Materials and methods

The alloys were prepared by milling elemental Fe, Co, Ni, B and prealloyed Zr–Ni powders (purity of 99.9% or more and particle size below 150 μm) in a planetary ball mill (Fritsch P7) using stainless steel balls and a vial with a ball-to-powder mass ratio of 5:1 in argon atmosphere. The milling process was performed at a speed of 700 rpm for 10, 20, 40 and 80 h. The alloys composition is: $Fe_{70-x}Co_xNi_{14}Zr_6B_{10}$ (x=0, 10 and 20) and labeled as A, B and C, respectively.

The sample thermal characterization using isochronal experiments was carried out by differential scanning calorimetry (DSC) under an argon atmosphere in a DSC822 equipment of Mettler-Toledo. The apparent mass changes on heating were analyzed using a thermogravimetry (TG) in a TGA851 Mettler Toledo equipment adapted with an small magnet as described in [15].

The morphology and composition study was performed by scanning electron microscopy (SEM) in a DSM960 A Zeiss equipment with energy dispersive X-ray microanalysis (EDX) and by induced coupled plasma (ICP) in a Liberty-RL ICP Varian equipment.

---

[*] Author for correspondence: joanjosep.sunyol@udg.es

1388–6150/$20.00

Akadémiai Kiadó, Budapest, Hungary
Springer, Dordrecht, The Netherlands

Results and discussion

Thermal study was performed by differential scanning calorimetry. Figure 1 shows the DSC scans of alloy A milled for 10, 20, 40 and 80 h. Milling process was performed until 80 h in order to obtain a nanocrystalline alloy. After 80 h of milling the nanocrystalline size of the bcc Fe(Co,Ni) phase, as determined by X-ray diffraction analysis, was 7.5 nm [16]. Similar values, 10.2 and 8.7 were found for alloys B and C, respectively. In essence, this nanoparticles size is close to where single-domain magnetic properties come into play [17]. As shown in Fig. 1, several exothermic processes were detected on heating. There is a broad hump beginning at about 400 K. The hump is associated with the relief of internal stresses, since no phase transformations were detected in X-ray diffraction and Mössbauer studies performed in alloys with similar composition [18, 19]. The two exothermic peaks over 600 K at 80 h MA correspond to the crystallization processes.

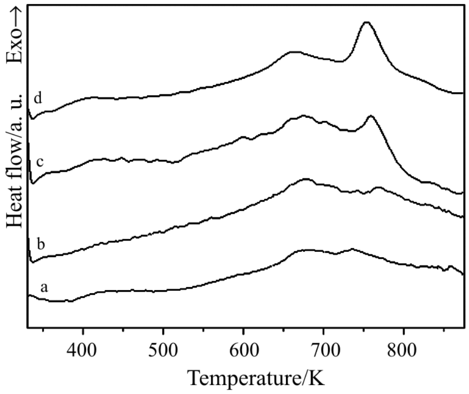

Fig. 1 DSC scans corresponding to alloy A milled for: a – 10, b – 20, c – 40 and d – 80 h. Heating rate: 10 K min^{-1}

Figures 2 and 3 show the DSC scans of alloys B and C, respectively. In these alloys, the low temperature relaxation process is less exothermic and the crystallization processes are more complex. The calorimetric data of alloy B milled for 80 h reveal a broad hump overlapped with a crystallization process in the temperature range of 500–750 K. The exothermic process over 750 K corresponds to the main crystallization process. As shown in Fig. 3, during heating the sample C milled for 80 h has also a complex crystallization shape, consequent with an inhomogeneous distribution of Co in the alloy. On increasing the Co content the first crystallization process shifts to lower temperatures and becomes less exothermic. On the contrary, the main crystallization process becomes more exothermic and is displaced to higher temperatures and complex in shape.

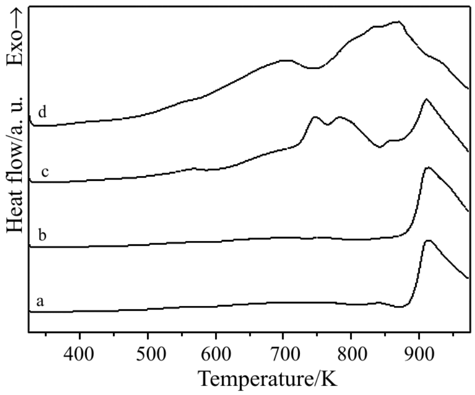

Fig. 2 DSC scans corresponding to alloy B milled for: a – 10, b – 20, c – 40 and d – 80 h. Heating rate: 10 K min^{-1}

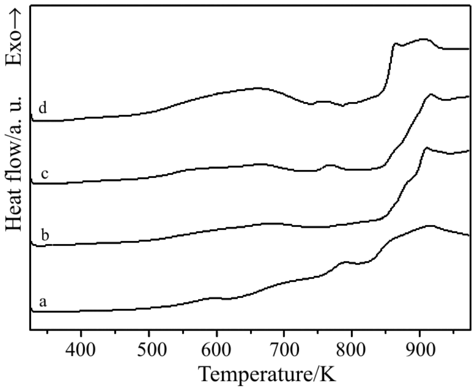

Fig. 3 DSC scans corresponding to alloy C milled for: a – 10, b – 20, c – 40 and d – 80 h. Heating rate: 10 K min^{-1}

To perform an evaluation of the activation energy, the crystallization data have been collected from DSC curves, obtained at different heating rates: 2.5, 5, 10, 20 and 40 K min^{-1}. The apparent activation energy, E, for the main crystallization process of alloys milled 80 h can be evaluated using the Kissinger equation [20] by linear fitting of $\ln(\beta / T_\mathrm{p}^2)$ *vs.* $1/T_\mathrm{p}$, with β the heating rate and T_p the peak temperature. The activation energy values are given in Fig. 4. In the case of the first crystallization process, the values vary between 1.4 and 1.5 eV at^{-1}. This broad exothermic process might be due to crystalline growth of the bcc Fe(Co,Ni) phase favored by the relief of internal stress [21, 22]. The main exothermic process over values, between 3.7 and 3.1 eV at^{-1} can reasonably be associated with a nucleation and grain growth process. Values between 3.1 and 3.9 eV at^{-1} were found in the bibliography of FeCo based alloys [23]. Similar behavior was found in nanocrystalline mechanically alloyed Fe–(Zr,Nb)–B–(Cu) alloys [19, 24]. In short, the introduction of Co induces the appearance of a complex crystallization behavior and a higher thermal stability against the main crystallization process. Complementary structural analysis is under study.

The thermomagnetic apparent mass (TGM) and their derivative (DTGM) of alloys milled for 80 h are

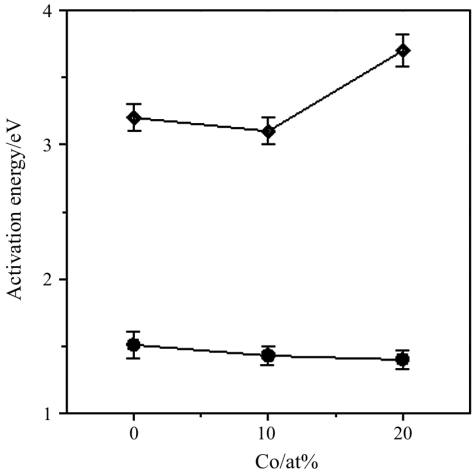

Fig. 4 Apparent activation energies obtained from Kissinger fits of the crystallization processes detected in DSC scan of alloys milled for 80 h

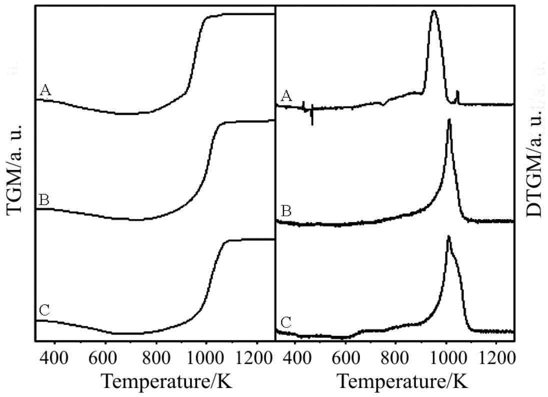

Fig. 5 The thermomagnetic apparent mass (TGM) and their derivative (DTGM) as a function of temperature

given in Fig. 5 as a function of temperature. The low temperature process produces a diminution of the apparent mass due to the microstructure rearrangements at the atomic level and to the strain relaxation. At higher temperatures (at about 900 K) the ferromagnetic-paramagnetic transition appears as a broad and complex process, as shown in the DTGM curve, indicating the transformation of different Fe-rich environments. The main result of the process is the change of the magnetic behaviour of the alloy provoked probably by the formation of the FCC paramagnetic phase. Since in experiments performed at high temperature the transition related to Co was not detected, it is concluded that Co is present in solid solution in the bcc Fe-rich phase.

The morphology of the powders was analyzed by scanning electron microscopy. Figure 6 shows three micrographs that correspond to the alloys after 80 h of milling. The as-milled powder has a relatively broad distribution of particle size, and most particles are found in the range of 2–40 μm, where higher particles corresponds to alloy with higher Co content. EDX microanalysis shows that big particles have the higher Co content (~12%) indicating the non-complete homogeneity of the alloy. The heats of mixing between Fe and Ni, Zr, B and Co are –3, –25, –38 and –1 kJ mol^{-1}, respectively [25]. Therefore, the mixing of Fe and Co at the atomic level is expected to be difficult in the solid-state [26] favoring the formation of different crystalline environments. When dealing with production of alloys by MA, it is necessary to control and evaluate the potential for significant contamination from the milling media (balls and vial) or atmosphere. In this sense, we have found traces of oxygen from oxides. This contamination is favored by the high surface/volume ratio of the small particles. The contamination measured by EDX and ICP in the powdered alloy increases with the milling time but remains always lower than 1.1 at%. Respect to the contamination by the milling tools (Fe, Ni and Cr), the results show only slight (<1.2 at%) contamination after 40–80 h of MA. As evaluated here, this influence is probably negligible when compared with the effect of Co addition.

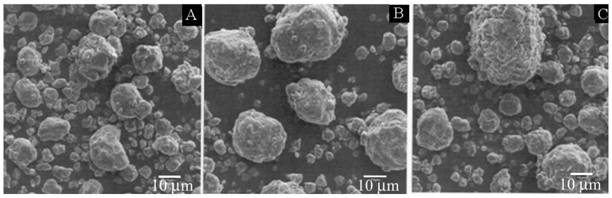

Fig. 6 SEM micrographs that correspond to the alloys milled during 80 h

Conclusions

Three nanocrystalline alloy, $Fe_{70-x}Co_xNi_{14}Zr_6B_{10}$ (x=0, 10 and 20), have been produced by mechanical alloying. The alloy milled for 80 h, consisted of metastable bcc-Fe(Co,Ni) nanocrystals. The calorimetric data reveal a broad hump beginning at about 400 K and two crystallization zones at higher temperature. The hump is associated with the relief of internal stresses. The first crystallization process, with activation energy (~1.4–1.5 eV at^{-1}) is associated to the growth of the bcc-Fe(Co,Ni) phase. The exothermic peak over 700 K corresponds to the main crystallization process. The apparent activation energy values, between 3.7 and 3.1 eV at^{-1} can reasonably be associated with the nucleation and grain growth process of a new phase. The partial substitution of Fe by Co produces higher thermal stability of the nanocrystalline alloy with respect to the main crystallization process.

Acknowledgements

Financial support from MICYT MAT2003-08271-C02-02 (FEDER) and DURSI 2005-SGR-00201 is acknowledged. J. B. agrees a Spanish FPI fellowship.

References

1 C. Suryanarayana, Progr. Mater. Sci., 46 (2001) 1.
2 K. Wieczorek-Ciurowa and K. Gamrat, J. Therm. Anal. Cal., 82 (2005) 719.
3 K. Wieczorek-Ciurowa, K. Gamrat and Z. Sawlowic, J. Therm. Anal. Cal., 80 (2005) 619.
4 T. Pradell, J. J. Suñol, N. Clavaguera and M. T. Mora, J. Non-Cryst. Solids, 276 (2000) 113.
5 M. E. McHenry, M. A. Willard and D. E. Laughlin, Progr. Mater. Sci., 44 (1999) 291.
6 K. Suzuki, N. Kataoka, A. Inoue, A. Makino and T. Masumoto, Mater. Trans. JIM., 31 (1990) 743.
7 J. van Wonterghem, S. Morup, C. J. W. Koch, S. W. Charles and S. Wells, Nature, 322 (1986) 622.
8 J. Shen, Z. Li, Q. Yan and Y. Che, J. Phys. Chem., 97 (1993) 8504.
9 D. Wexler, R. Bennett, M. Emr and K. P. Gillerad, Mater. Sci. Forum, 235–238 (1997) 729.
10 Y. I. Jang, J. Kim and D. H. Shin, J. Mater. Sci. Eng. B, 78 (2000) 113.
11 A. González, J. J. Suñol, J. Bonastre, L. Escoda and J. Caleya, J. Therm. Anal. Cal., 80 (2005) 253.
12 S. Linderoth and S. Morup, J. Appl. Phys., 69 (1991) 5256.
13 H. Chiriac, A. E. Moga, M. Urse and C. Hison, J. Metastable Nanocryst. Mater., 8 (2000) 806.
14 J. J. Suñol, N. Clavaguera and M. T. Mora, J. Non-Cryst. Solids, 287 (2001) 114.
15 J. J. Suñol, A. González, L. Escoda and A. Vilaró, J. Therm. Anal. Cal., 80 (2005) 257.
16 J. J. Suñol, T. Pradell, N. Clavaguera and M. T. Clavaguera-Mora, Philos. Mag., 83 (2003) 2323.
17 B. D. Cullity, Introduction to Magnetic Materials (Addison-Wesley Publishing Company, 1972).
18 J. J. Suñol, T. Pradell, N. Clavaguera and M. T. Clavaguera-Mora. Mater. Sci. Forum, 360 (2001) 525.
19 J. J. Suñol, A. González, J. Saurina, L. Escoda and P. Bruna, Mater. Sci. Eng. A, 375 (2004) 874.
20 H. Kissinger, Anal. Chem., 29 (1957) 1702.
21 A. Calka and A. P. Radlinski, Acta Metall., 35 (1987) 1823.
22 M. T. Clavaguera-Mora, J. J. Suñol and N. Clavaguera, J. Metastable Nanocryst. Mater., 10 (2001) 459.
23 J. S. Blázquez, C. F. Conde and A. Conde, J. Non-Cryst. Solids, 287 (2001) 187.
24 M. Multigner, A. Hernando, P. Crespo, C. Stiller, J. Eckert and L. Schultz, J. Magn. Magn. Mater., 197 (1999) 214.
25 F. R. de Boer, R. Boom, W. C. M. Mattens, A. R. Miedema and A. K. Niessen, Cohesion in Metals, North-Holland, The Netherlands 1989, p. 230.
26 Y. J. Liu, I. T. H. Chang and P. Bowen, Mater. Sci. Eng. A, 304–306 (2001) 383.

DOI: 10.1007/s10973-006-7802-0